

SEMI-AUTOMATIC SIGN BOARD RECONSTRUCTION FROM A LAND VEHICLE MOBILE MAPPING SYSTEM

Yu-Chun Yen^a, Po-Chia Yeh^a, Jiann-Yeou Rau^b
^aGraduate Student and ^bAssistant Professor

Department of Geomatics, National Cheng Kung University
 No.1 University Road, Tainan City 701, TAIWAN;
 Tel: +886-6-2757575~63839;

E-mail: yuady@msn.com, ypcsogoodshot@gmail.com, jiannyourau@gmail.com

KEY WORDS: Sign board detection, Line segmentation detection, Space intersection.

ABSTRACT: There is lots of semantic information in the sign board related to its corresponding building. For example, we can realize the property of the shop via the sign board. Previous study on sign board detection and recognition from mobile mapping system (MMS) is rare. However, if this process could be done automatically, it will increase the efficiency for POI (point of interest) collection. In this paper, we capture the street view images from a land vehicle MMS, which was configured with three stereo cameras by viewing the front of car and two street sides. At first, we detect straight line-segments by an open source called Line Segmentation Detector (LSD) and perform semi-automatic line-segment matching, then using line-plane intersection algorithm for space intersection to obtain the sign board boundary on the object space. Finally, we perform geometrical reconstruction to get 3D model of the sign board, based on the assumption that the sign board is made in a thin plate. In this study, some factors affect the line segment detection will be analyzed, such as shadow, occlusion, and shape of the sign board, image resolution, and geometric distortion introduced by cameras' viewing angles. Experimental results show that the above mentioned effects will decline the successful rate; particularly the shape of sign board must be complete and clear. Meanwhile, the scale change within the image will introduce spatial resolution variation, thus further studies are necessary to cope with those deficiencies in order to increase the success rate, reliability and robustness. Nevertheless, two successful examples will be illustrated to demonstrate its potential in POI collection.

1. INTRODUCTION

Land-based Mobile mapping system (MMS) is vigorous developed and widely applied in the fields of Navigation, Photogrammetry and GIS. It can be applied in city planning, road infrastructure inventory, POI collection, car navigation, etc. When we need to link the location and attribute, it can obtain data in a short time. Signboard is important for users since it contains lots of semantic information. The mobile mapping system (MMS) we used is a land-based vehicle that equipped with six cameras (three stereo-pairs) as well as GPS, IMU and Odometer (Rau et al., 2011). We collect the images first and perform line segment detection on it. Then we adopt manual line-matching for acquiring 3D structural lines and reconstruct the sign boards. Finally, we perform texture mapping to create the texture of sign boards.

For edge detection, some edge detectors are widely used, such as Canny edge detector (Canny, 1986), Hough Transform (Gonzalez and Woods, 1993), Line Segment Detector (Von Gioi et al., 2010), etc. The main parameter of Canny edge detector is the Gaussian scale, the lower value brings less blur effect on image. We need adjust this value depends on the imagery content and this method detect lots of edges on tree area. For Hough Transform, the advantage is anti-noise, but the disadvantage is each scene has its own threshold. The line detection algorithm used in this paper is the Line Segment Detector (LSD) (Von Gioi et al., 2010), it is adaptive to the geometric transformation and rotation. Meanwhile, it can deal with lots of imagery in a short time and obtain reliable results without adjusting the parameters.

2. METHODS AND EQUATION

Figure 1 shows the flow chart of our method. We present a method to reconstruct the signboard texture from a land vehicle mobile mapping system. We assume the signboards are formed by rectangular polygons. The camera lens was calibrated within the laboratory to obtain the interior orientation parameter (IOP). For the purpose of direct georeferencing the boresight and lever arm have to be calibrated to obtain all images' exterior orientation parameters (EOP). Subsequently, we detect the image line segment by LSD and perform multiple images line matching manually. Later, a space intersection algorithm based on line-plane intersection is applied to obtain 3D structural lines, then we can estimate four vertices of the signboard boundary to reconstruct the signboard.. Finally,

those vertices can be back-project onto the original image to perform texture mapping.

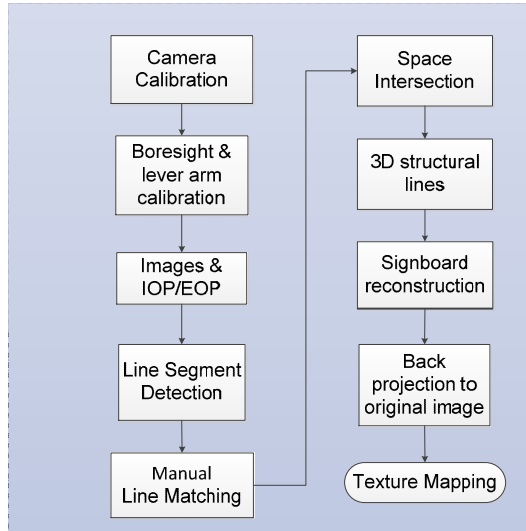


Figure 1. Flow Chart of Sign Board Reconstruction

2.1 Direct Georeferencing

Figure 2 illustrated the adopted land vehicle MMS, in which a medium-cost tactical grade MEMS GPS/INS integrated POS system is adopted (SPAN-CPT and a NovAtel © ProPak-V3 GPS receiver). The positional accuracy of such POS system after post-processing, in case of no GPS outage and using kinematic GPS data collection, is about 10 cm for the horizontal direction and 15 cm for the vertical, and the accuracy of the integrated GPS/INS attitude is 0.05° for the roll and pitch and 0.1° for the heading, which is satisfactory for many applications and its cost is quite low when compared to a strategic grade IMU and the Applanix © POS AV 510, for example.

The concept of Direct Georeferencing (DG) is shown in figure 3. This research adopts DGPS positioning with a base station and a tightly-coupled scheme that integrates the IMU and GPS measurements to provide a seamless POS-based solution for direct sensor orientation. The idea is to overcome the disadvantages of the conventional loosely-coupled system. When the number of GPS satellites is less than four, a tightly-coupled scheme is still able to provide integrated navigation solutions through the GPS measurements update. The adopted scheme is particularly suitable for a congested urban environment where GPS signal is frequently obscured. For boresight and lever-arm calibration, since the adopted MMS is a multi-camera system, the mounting parameters comprise two sets of Relative Orientation Parameters (ROPs), i.e. the ROPs among the cameras as well as the ROPs between the cameras and the navigation sensors. A detail calibration procedure can be found in Rau et al. (2011).



Figure 2. The adopted land vehicle MMS.

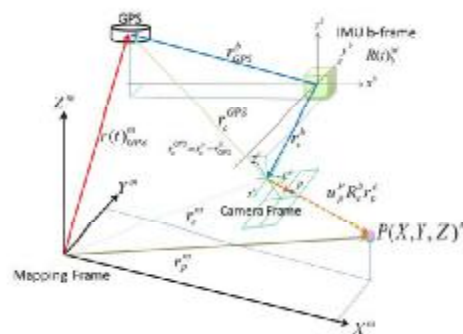


Figure 3. The Concept of Direct Georeferencing

2.2 Line Segment Detector

Line segment detector (LSD) (Von Gioi et al., 2010) is an open source code. It calculates the gradient value and direction first. Using the threshold ρ , the pixels with small gradient value will be excluded. Others using region

growing instead. Figure 4 shows the region growing steps. The dash line is direction of gradient and the blue point is growing pixels. It starts from a seed point and search the neighboring pixels. It needs a threshold τ , the smaller the τ , the over segments will be appear. Meanwhile, we can get a complete segment when the τ is lager, but it can't detect the related points. It is suggested that the τ is set as 22.5 degree and it can get the best result.

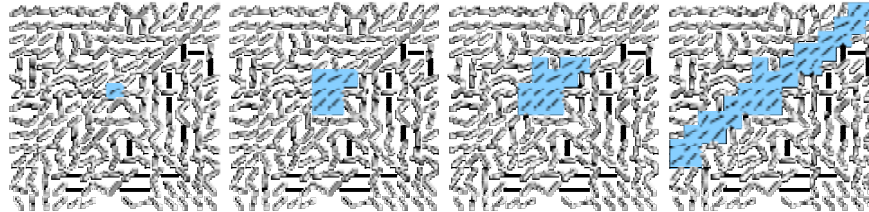


Figure 4. Region Growing (Von Gioi et al., 2010)

The pixel with the biggest gradient value is the starting pixel because these pixels have the characters of edges. The larger gradient value of pixel is more probably to be the line edge. Each pixel is one seed point. We won't use this point in the same rectangle after adding this seed point. It means each pixel only belongs to one line segment and each segment in an image is independent. Region growing of LSD extend ultimately when it didn't exceed the threshold. Any point can get one straight line. On the contrary, it might effect on the starting point when the edge is curve. The result of the curve is a combination of several straight lines. The advantage of this method is that it can adaptive to any image without the need to adjust thresholds. The disadvantage is that it can't detect curve accurately.

2.3 Manual Line Segment Matching

Automatic multiple line segments matching is very important step for 3D polyhedral model reconstruction. It often occur some problems such as occlusion, shadow, repeat pattern and so on. The objective of this study is to create signboard boundary's 3D structural line based on the detected line segments and to evaluate the feasibility of the proposed procedure, not the line matching. Thus, a multiple lines manual matching scheme is suggested instead. In the experiment, we develop a windows-based GUI interface as illustrated in figure 5 to realize the whole procedure. We can shift, zoom in/out and overlap the line segment through this system. We choose the images taken on different locations and select the conjugate lines manually (as shown in yellow in figure 5). Then, we can obtain 3D structural lines via line-plane space intersection and reconstruct the signboard's shape.



Figure 5. A windows-based GUI for manual multiple lines matching.

2.4 Line-Plane Space Intersection

The concept of line-plane space intersection is to reconstruct the 3D object coordinates by collinear equations and one line-segment on the image plane will create an infinite plane. It requires the coordinates of endpoints of the line segment. For example, in figure 6, A1 and A2 are two endpoints of a line segment. Combining camera's perspective center O1, an infinite plane is generated. Line segment A1'-A2' is the conjugate line on the second image. O2-A1' is a vector (line) that will intersect with the plane O1-A1-A2 to obtain one 3D object point corresponding to A1'. Consequentially, for two images a total of four object points are obtained. Later a line-fitting based on Singular Value Decomposition (SVD) is used to construct a single 3D structural line. In the following is the procedure for

line-plane intersection.

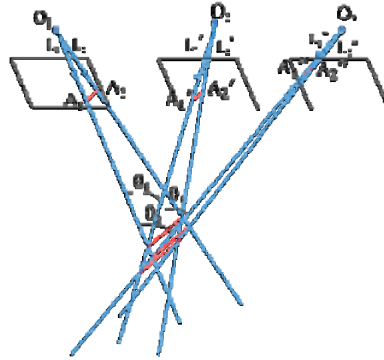


Figure 6. Line-Plane Intersection

First of all, we utilize the collinearity equations to obtain the coordinate of image point in the object coordinate system.

$$\vec{v}_i = \lambda M(\omega, \phi, \kappa) \vec{V}_0 \quad (1)$$

$$\begin{bmatrix} x_a - x_p \\ y_a - y_p \\ -f \end{bmatrix} = \lambda \begin{bmatrix} m_{11} & m_{12} & m_{13} \\ m_{21} & m_{22} & m_{23} \\ m_{31} & m_{32} & m_{33} \end{bmatrix} \begin{bmatrix} X_A - X_0 \\ Y_A - Y_0 \\ Z_A - Z_0 \end{bmatrix}$$

Where \vec{v}_i = vector in the image space.

- M = rotation matrix
- f = focal length
- x_a, y_a = image coordinate
- x_p, y_p = principal point
- X_A, Y_A, Z_A = object coordinate in the object coordinate system
- X_0, Y_0, Z_0 = coordinates of projection center

After we get the object coordinate, we utilize the plane equation (2). Just like the figure 6 shows, the $O_1, A_1,$ and A_2 belong to the same plane.

$$AX + BY + CZ + D = 0 \quad (2)$$

Where X, Y, Z are object coordinates in the object coordinate system.

The line is formed with two points, the line equation in the right image $\overline{O_2A_1'}$ can be represented by formula (3) in parametric form.

$$\begin{aligned} x &= X_2 + (X_{A1'} - X_2)t \\ y &= Y_2 + (Y_{A1'} - Y_2)t \\ z &= Z_2 + (Z_{A1'} - Z_2)t \end{aligned} \quad (3)$$

We can get the intersected point P (x_p, y_p, z_p) (as shown in figure 7) by formulas (4) and (5).

$$\begin{aligned} x &= x_0 + at \\ L \sim y &= y_0 + bt \quad K : Ax + By + Cz + D = 0 \\ z &= z_0 + ct \end{aligned} \quad (4)$$

$$\begin{aligned} x_p &= x_0 - \frac{a(Ax_0 + By_0 + Cz_0 + D)}{Aa + Bb + Cc} \\ y_p &= y_0 - \frac{b(Ax_0 + By_0 + Cz_0 + D)}{Aa + Bb + Cc} \\ z_p &= z_0 - \frac{c(Ax_0 + By_0 + Cz_0 + D)}{Aa + Bb + Cc} \end{aligned} \quad (5)$$

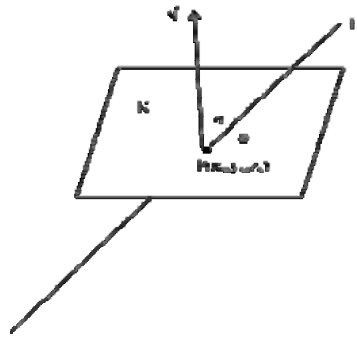


Figure 7. Line-Plane Intersection

We can acquire the O_1, O_2 object coordinates after formula (2) and (3). On the other hand, for the right image another plane and line are formed with image point (A_1' & A_2') as well as its perspective center O_2 . We can get 4 intersection points after line-plane intersection through those two images. We can obtain 12 intersection points by taking 3 plane (3 images) into account.

2.5 Line Fitting

The concept of least squares line fitting is to fit all observations as a line and lead to a minimal of summation of residuals squares. For 3D line equation, some errors in the observation could cause divergence. To avoid this problem, a total least squares method that allows some blunders in the observation and coefficient matrix is suggested. This is particularly useful when small intersection angles occurred. In this study, we use Singular Values Decomposition (SVD) to solve this problem. If we have number of m point (x_i, y_i, z_i) , $m > 2$, the line L can be represent as (6)

$$\begin{aligned} x &= x_0 + at \\ y &= y_0 + bt \\ z &= z_0 + ct \end{aligned} \tag{6}$$

Where (a,b,c) are directional vector of line L . (x_0, y_0, z_0) is any point through L . We find the center point P_0 first by equation (7), because the center point is very close to the best fitted line.

$$\begin{aligned} \bar{x} &= \sum_{i=1}^n x_i / n \\ \bar{y} &= \sum_{i=1}^n y_i / n \\ \bar{z} &= \sum_{i=1}^n z_i / n \end{aligned} \tag{7}$$

Using the SVD to calculate the directional vector (a, b, c) .

$$A = \begin{bmatrix} x_1 - \bar{x} & y_1 - \bar{y} & z_1 - \bar{z} \\ \vdots & \ddots & \vdots \\ x_n - \bar{x} & y_n - \bar{y} & z_n - \bar{z} \end{bmatrix} \tag{8}$$

Where A is the design matrix, we can transform it into two orthogonal matrix and characteristic diagonal matrix. The smallest singular values corresponding to the base vector is the required solution (a,b,c) .

2.6 3D Structural Lines Intersection

As mentioned earlier, we assume the signboard is represented as a rectangular polygon that can be reconstructed by four 3D structural lines. Based on previous detected 3D structural lines we can estimate the 3D coordinate of the polygon's four vertices. It means that from two neighbored 3D structural lines we can obtain one vertex by line intersection as depicted in figure 8. Generally, two 3D structural lines cannot intersect (touch) to each other, thus a line perpendicular to both lines is calculated and its middle point is treated as the intersection point.

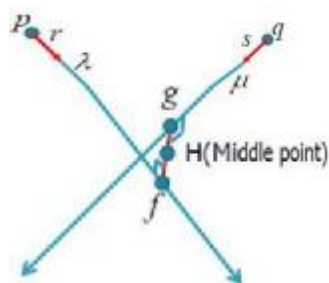


Figure 8. Middle Point through Two Linear Parametric

2.7 Back Projection & Texture Mapping

We know the EOPs/IOPs of the images and cameras respectively, so we can get the image coordinates of all four signboard's vertices by back projection using the collinearity equations. An example is depicted in figure 9. Further, we can interpolate the color from the original image to obtain a rectified image (texture) for the signboard. However, from figure 9 one may find out sometimes the signboard maybe occluded by the other objects. In this study, we decide the best one by visual inspection. A further study to automate the whole decision process is required.

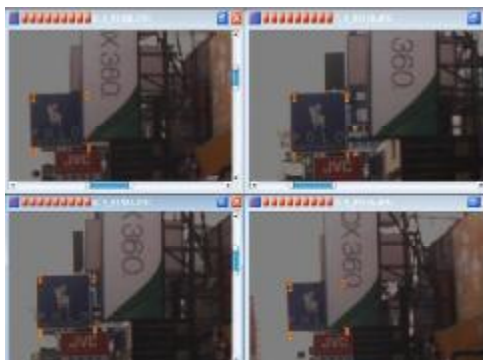


Figure 9. Back projection results.

3. RESULTS

The purpose of this study is to verify the proposed procedure and concept, thus only preliminary analysis and two examples are demonstrated.

3.1 Visual Qualitative Analysis

The original image is 1624*1234 and the number of the line segments detected is about 4000. As shown in figure 10, LSD is suitable for straight line. If the target is in circle, the result is a combination of several line segments. Thus, in this study only rectangular signboards are used for experiment.



Figure 10. Result of LSD for a circular shape signboard.

3.2 Accuracy analysis of LSD

For this purpose, we simulate 6 images with different Gaussian blur and Gaussian noise effects. Then, detect the line segments through LSD. As shown in figure 11, the image contains two diagonal line segments (1 & 2) and four colors. The detected line segments were drawn in yellow. Table 1 tabulated the position and orientation errors after LSD. It demonstrated that under the assigned blur and noise effects, the detected line segments can have an orientation error less than 0.1° and positional error less than 0.6 pixels. It shows that LSD is an accurate and useful tools for line segment detection and suitable for our demand.

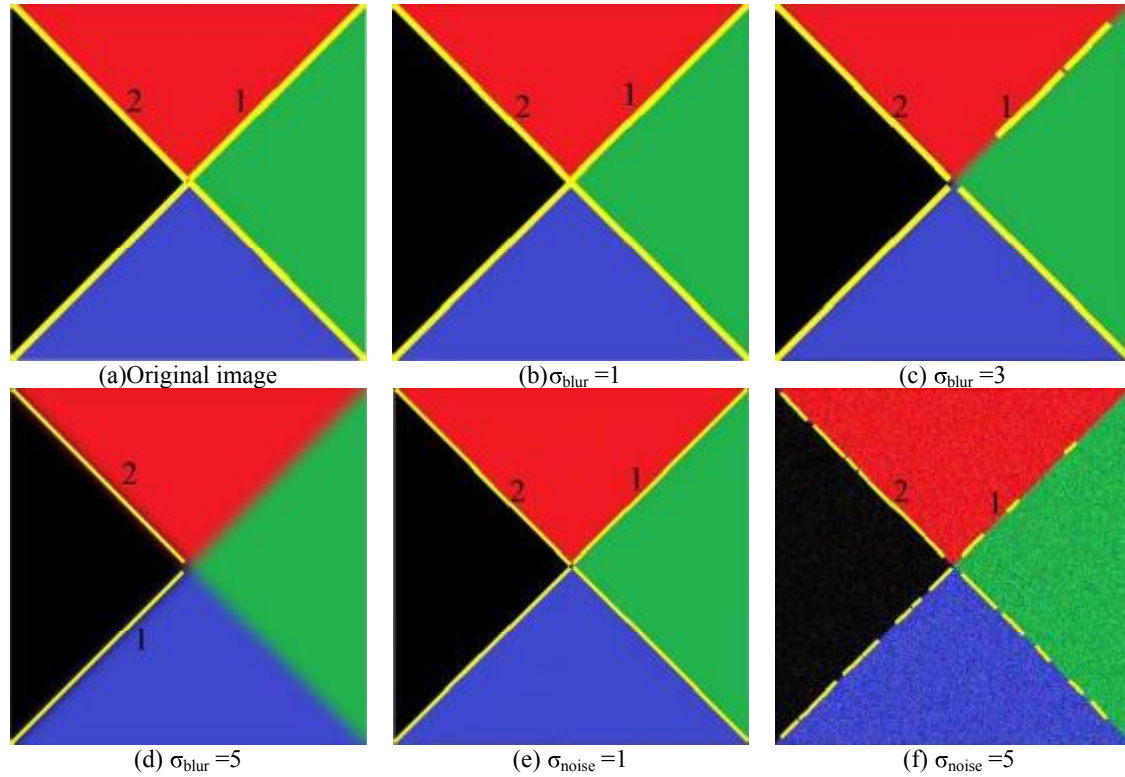


Figure 11. Performance test of LSD

Table 1. Accuracy Evaluation of LSD

	Segment 1		Segment 2	
	slope(degree)	intercept(pixel)	slope(degree)	intercept(pixel)
Original	0.02°	0	0°	0.32
$\sigma_{\text{blur}}=1$	0°	0.02	0.01°	0.34
$\sigma_{\text{blur}}=3$	0.01°	0.05	0.01°	0.23
$\sigma_{\text{blur}}=5$	0.02°	0.17	0.01°	0.25
$\sigma_{\text{noise}}=1$	0.05°	0.20	0.06°	0.33
$\sigma_{\text{noise}}=5$	0.09°	0.29	0.03°	0.6

3.3 Signboard reconstruction

Generally, the signboard is vertical but some are extruded from the façade and some attached on the wall. In this case study, both of them are test as shown in figure 12 with red and yellow circles. Since the wall is parallel to road, thus generally the signboard on the wall will be distorted more serious than the extruded one. After applying the proposed procedure, we obtain the 3D structural lines of the signboard's boundary and estimate their 3D vertices coordinates. Then, we can get the image point on the image coordinate by back projection and apply texture mapping. The final results were depicted in figures 13(a) and 13(b).

4. CONCLUSIONS & RECOMMENDATIONS

We detect line segment first and perform multiple lines matching manually. Secondly, a space intersection algorithm based on line-plane intersection is applied to obtain 3D structural lines. Finally, we use back projection and texture mapping to get the signboard. From the experiment and case study, we conclude that (1) the DG result is crucial during the space intersection for obtaining the 3D structure of signboard. (2) The suggested LSD is suitable for straight line extraction. (3) A longer line segment has better reliability during 3D structural line reconstruction. (4) A larger line-plane intersection angle can obtain more accurate and reliable space intersection results. (5) The proposed signboard reconstruction procedure has high potential in fully automatic signboard reconstruction. Further studies are required to automate the whole procedure, such as automatic multiple lines matching, particularly under occlusion situation and shadow effect.



Figure 12. Case studies



(a) Extruded signboard



(b) Signboard on a wall

Figure 13. Experiment Results

ACKNOWLEDGEMENT

This research was, in part, supported by the Ministry of Education, Taiwan, R.O.C. The Aim for the Top University Project to the National Cheng Kung University (NCKU). The project is also partially sponsored by the National Science Council (NSC), Taiwan. The authors are grateful for their support.

REFERENCES

Canny, J., A Computational Approach To Edge Detection, IEEE Trans. Pattern Analysis and Machine Intelligence, 8(6):679-698, 1986.

Gonzalez, R.C. and Woods, R.E., Digital Image Processing, Prentice Hall, 1993

Rau, Jiann-Yeou & Po-Chia Yeh, "A Semi-Automatic Image-Based Close Range 3D Modeling Pipeline Using a Multi-Camera Configuration", Sensors, 12(8), pp. 11271-11293.

Rau, Jiann-Yeou, Ayman F. Habib, Ana P. Kersting, Kai-Wei Chiang, Ki-In Bang, Yi-Hsing Tseng and Yu-Hua Li, 2011, Direct Sensor Orientation of a Land-Based Mobile Mapping System, Sensors, 11(7), pp.7243-7261.

Von Gioi, R.G., Jakubowicz, J., Morel, J.M., Randall, G., 2010. LSD: A fast line segment detector with a false detection control. Pattern Analysis and Machine Intelligence, IEEE Transactions on 32, 722-732. http://www.ipol.im/pub/alg/gjmr_line_segment_detector